



# Study of AlSi9Cu3 Alloy Crystallization Process with Increased Iron Content at Different Number of Remelts

M. Matejka<sup>a,\*</sup>, D. Bolibruchova<sup>a</sup>, J. Kasińska<sup>b</sup>, M. Kuriš<sup>a</sup>

<sup>a</sup>Department of Technological Engineering, University of Zilina,  
 Univerzitna 1, 010 26 Zilina, Slovak Republic

<sup>b</sup>Kielce University Technology, Faculty of Mechatronics and Mechanical Engineering,  
 Department of Metal Science and Manufacturing Processes,  
 Al. Tysiąclecia P.P.7, 25-314 Kielce, Poland

\* Corresponding author. E-mail address: marek.matejka@fstroj.uniza.sk

Received 03.08.2019; accepted in revised form 03.10.2019

## Abstract

Monitoring the solidification process is of great importance for understanding the quality of the melt, for controlling it, and for predicting the true properties of the alloy. Solidification is accompanied by the development of heat, the magnitude of which depends on the different phases occurring during solidification. Thermal analysis is now an important part of and tool for quality control, especially when using secondary aluminium alloys in the automotive industry. The effect of remelting on the change of crystallization of individual structural components of experimental AlSi9Cu3 alloy was determined by evaluation of cooling curves and their first derivatives. Structural analysis was evaluated using a scanning electron microscope. The effect of remelting was manifested especially in nucleation of phases rich in iron and copper. An increasing number of remelts had a negative effect after the fourth remelting, when harmful iron phases appeared in the structure in much larger dimensions.

**Keywords:** Al-Si-Cu, Remelting, Thermal analysis, Structural analysis

## 1. Introduction

Al-Si-Cu-based alloys are still among the frequently used materials in the foundry industry. They are being used due to their low weight and good resulting properties of components. They are mainly used in the production of cylinder heads and engine blocks, wardrobes and other components where one of the basic requirements is the tightness of the castings [1].

One of the most commonly used alloys of this type is the AlSi9Cu3 alloy. This alloy is usually produced as a secondary type of alloys, i.e. by remelting various materials - returnable

foundry materials, returnable materials from forming processes, non-conforming castings, gating and runner systems, etc [1, 2].

In determining the mechanical and physical properties, the chemical composition is as important as the microstructure and utility properties. Chemical analysis of the alloy determines the presence of elements in the melt. Nevertheless, it will not indicate the phases that occur during solidification, especially during casting. These phases can be identified when evaluating the thermal analysis. The temperature changes in the solidification process from liquidus temperature to solidus temperature are related to microstructural changes such as seeding and eutectic silicon modification [3]. Microstructure is important in cast aluminum alloys because it has a direct impact on the resulting

foundry and mechanical properties. The different parts of the solidification curve contained in the thermal analysis can be related to two microstructural properties. Nucleation or solid-crystal formation from the liquidus phase depends on the particles available as nucleation nuclei [3, 4].

The solidification of Al-Si-Cu alloys as well as the thermal analysis curve consist of three main parts. The first part is associated with the formation of small solid particles of the primary  $\alpha$ -phase (liquidus temperature). This temperature defines the transformation between the liquid and solid state of the alloy. Two - liquid and solid - phases occur simultaneously in the transition region. As the temperature decreases, the volume of the liquidus phase decreases and the solidus phase increases, and the primary precipitation of the Al-Si eutectic begins. In the final part, the copper-rich eutectic phases precipitate. If there is a sufficient amount of impurities in the alloy, e.g. based on iron, they can be analyzed on the solidification curve [4, 5].

It is the increased presence of iron as an impurity that is characteristic for remelted alloys. Iron together with other elements form intermetallic phases, e.g.  $Al_2Fe_3Si_2$  and in particular  $Al_3FeSi$  present in needle morphology negatively affect the resulting properties of the alloy [6].

Copper in this system lowers the liquidus temperature and worsens ductility, improves machinability and thermal conductivity. The biggest disadvantage is the reduced resistance to corrosion (intercrystalline type of corrosion), where the main catalyst is the presence of copper and the impact of the environment. There are no ternary compounds in the system [5, 7].

## 2. Experimental method

In terms of the experiment, there was a targeted increase (the so-called controlled pollution) in wt. % Fe in AlSi9Cu3 experimental alloy. The chemical composition of the alloy is shown in Tab. 1. The resulting iron quantity of 1.4 wt. % exceeds the maximum iron level 1.1 wt. % specified by the standard EN 1706 on purpose.

Multiple remelting consisted of casting ingots into prepared metal molds. After solidification and cooling, the ingots were used as a batch for further melting without additional chemical treatment. This process was repeated 6 times and the samples were refilled from the first melting (D1 as reference sample - no remelting) and from every other melting (D3 - after the third remelting, D5 - after the fifth remelting, D7 - after the seventh remelting) into the metal mold with a minimum temperature of  $100 \pm 5$  °C. The melting was carried out in an electric resistance furnace and the casting temperature was in the temperature range of 750 to 770 °C. The total batch weight was 15kg and melt was not vaccinated, modified or refined.

The process of crystallization of alloys with different degree of remelting was evaluated by thermal analysis. A K-type (NiCr-Ni) thermocouple placed in the center of a cylindrical metal mold with a diameter of 34 mm and a height of 50 mm was used during the measurement. Values were recorded in LabView 2 Hz program. Cooling curves and their first derivatives were generated from the measured values in order to accurately determine the

characteristic temperature for crystallization of the individual structural components of the alloy.

## 3. Results and Discussion

During cooling of the melt in the mold the temperature drops, which leads to the elimination of intermetallic phases. The solidification of all aluminum alloys begins at the liquidus temperature by the formation of small solid particles of the primary  $\alpha$ -phase. This temperature defines the first transformation between the liquid and solid state of the alloy. By contrast, the solidus temperature determines when the last liquid particle is transformed into a solid. Individual phase transformations occur at a specific temperature and are accompanied by heat release.

On the basis of the cooling curves and their first derivatives (Fig. 1), the characteristic transformation temperatures of the AlSi9Cu3 secondary alloy with different degree of remelting were determined. These temperatures are shown in Tab. 2. The gradual remelting of the alloy had no major effect on the change in liquidus (crystallization of phase alpha) and solidus temperatures as temperature at the end of solidification process. Liquid temperature ranges from 628 to 632 °C and solid from 474 to 478 °C, thus there is no significant change of the solidification interval of experimental alloys. In Fig. 1, there is a comparison of curves characterizing the proportion of solid and liquid phase depending on temperature. These curves were obtained based on the Linear and Scheil equations and Lever's rule [8, 9].

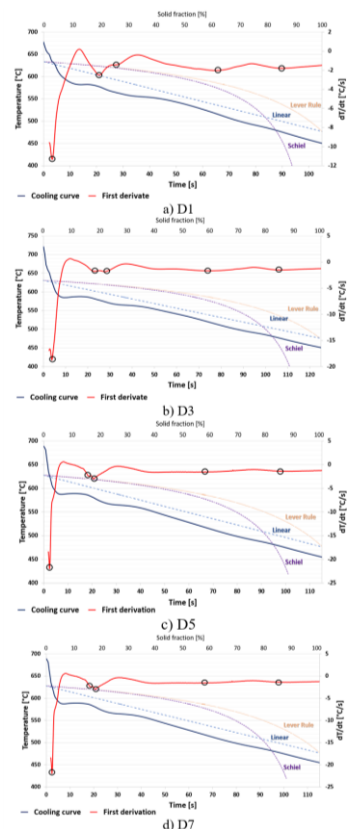


Fig. 1. Cooling curve and its first derivate of secondary alloy

Table 1.

Chemical composition of the AlSi9Cu3 alloy

Elements (wt. %)	Si	Fe	Cu	Mn	Mg	Ti	Cr	Sr
AlSi9Cu3	9.559	1.081	1.893	0.184	0.426	0.038	0.027	<0.002

### Precipitation of iron-rich phases

Multiple remelting of the experimental alloy led to a gradual increase in wt. % of iron, thus the value of  $Fe_{crit}$  in all alloys (Table 2) was exceeded. Exceeding the  $Fe_{crit}$  value caused that the iron-rich phases were eliminated first before the eutectic silicon phases, as shown in Fig. 2. The iron intermetallic phases that are formed prior to the crystallization of the AlSi eutectic tend to form phases of much larger dimensions than those formed after the eutectic solidifies. Weight increase of % Fe in the alloy led to an increase in the nucleation temperature of the iron phases. For reference alloy (D1), the nucleation temperature is  $T_{AlSiFe} = 578$  °C, while for the alloy after the sixth remelting (D7),  $T_{AlSiFe} = 585$  °C. From the curves of the first derivative, a gradual increase in the peak of the curve is visible in the region characterized by the formation of iron-rich phases, indicating that at a higher wt. % of Fe, more latent heat is released during crystallization of these phases.

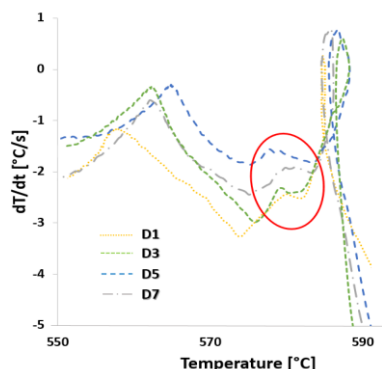


Fig. 2. Iron rich phases detected using first derivative curves of AlSi9Cu3 alloys in various degree of remelting

The iron rich phases in reference alloy D1 are eliminated mostly in needle-like morphology with an average needle length of 55.7  $\mu\text{m}$ . The needles are evenly distributed in the interdendritic regions (Fig. 3a). The paradox is that due to double remelting, the average lengths of iron needles in the D3 alloy were shortened. Probably due to remelting, long needles were 'broken' into phases with smaller dimensions. At D3 alloy, the needles reached an average of 37.8  $\mu\text{m}$ . The alloy structure after the fifth remelting of D5 is already expected to be characterized by a large number of needles of ferrous phases with an average length of 71.4  $\mu\text{m}$  (Fig. 4b). Subsequent application of the other two remelts, the average needle length still increased to 89.4  $\mu\text{m}$  (the alloy after the sixth remelting D7). Fig. 3b and 4b show details of the needles of the iron phases.

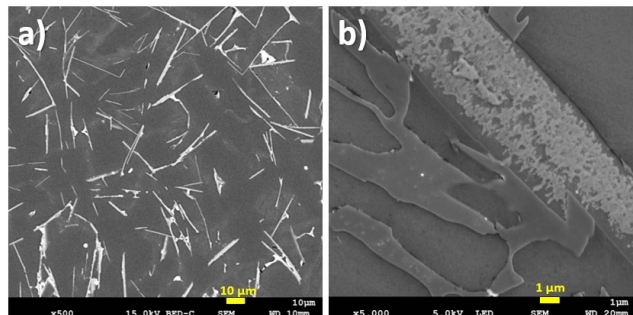


Fig. 3. Intermetallic iron-based phases in reference alloy D1, SEM a) distribution of phases b) detail of needle particles

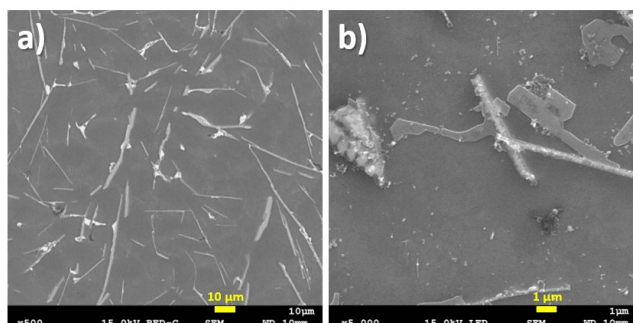


Fig. 4. Intermetallic iron-based phases in in alloy after 5<sup>th</sup> remelting D5, SEM a) distribution of phases b) detail of needle particles

Fig.5 shows a point EDX analysis of the needle phase, which confirmed the presence of higher iron content together with the elements Al and Si - it is the iron phase  $\beta$  -  $Al_5FeSi$ .

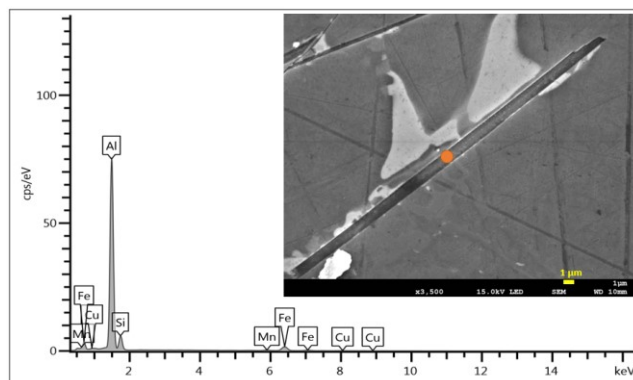


Fig. 5. EDX analysis of needle particles  $\beta$  -  $Al_5FeSi$  phase in alloy after 7<sup>th</sup> remelting D7

Table 2.

Characteristics of wt. % of selected elements, temperature of reaction and average length of iron phases of AlSi9Cu3 alloy with various degree of remelting

Alloy	Si [wt. %]	Fe [wt. %]	Cu [wt. %]	Fe <sub>crit</sub> [wt. %]	STR [°C]	T <sub>AlFeSi</sub> [°C]	T <sub>AlSi</sub> [°C]	T <sub>AlCu</sub> [°C]	Average length of iron phases [μm]
D1	9.347	1.416	1.741	0.651	632 - 478	578	569	515	55.7
D3	9.306	1.51	1.726	0.648	629 - 476	582	571	517	37.8
D5	9.302	1.705	1.667	0.647	628 - 477	584	574	520	71.4
D7	9.179	1.889	1.663	0.638	630 - 474	585	573	518	89.4

### Precipitation of copper-rich phases

Fig. 6. captures the area of crystallization of the copper-rich phase in more detail. It can be seen that even small changes in the Cu content due to remelting affect their nucleation. Depending on the amount of Cu and some other alloying elements such as Sr, Pb and Sn [10], the starting and final solidification temperatures of these phases may vary. The shape and size of the peaks visible in the Cu-enriched region on the first derivative temperature-dependent curves show that the amount of latent heat released during crystallization increased slightly after two remelts and then got stabilized at approximately the same level.

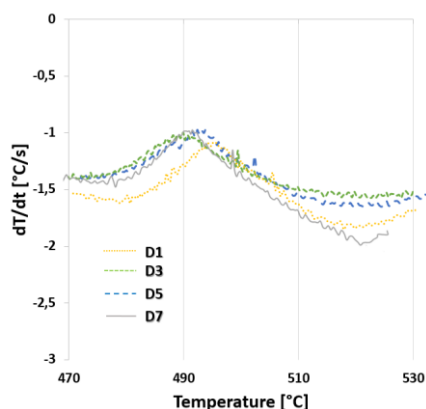


Fig. 6. Copper rich area of precipitation; The first derivative of the AlSi9Cu3 alloys in various degree of remelting cooling curves related to copper enriched region

Intermetallic phases rich in copper in all experimental alloys are primarily eliminated in the vicinity of eutectic silicon grains and, in particular, iron phase needles. The microstructure images of the alloy after the fourth remelting D5 (Fig. 7) present a more detailed view of the way of distribution of the copper phases in the area of the  $\beta$  - Al<sub>5</sub>FeSi phase needles. For a more comprehensive view of this area, an element mapping (Fig. 8) and line EDX analysis were performed (Fig. 9).

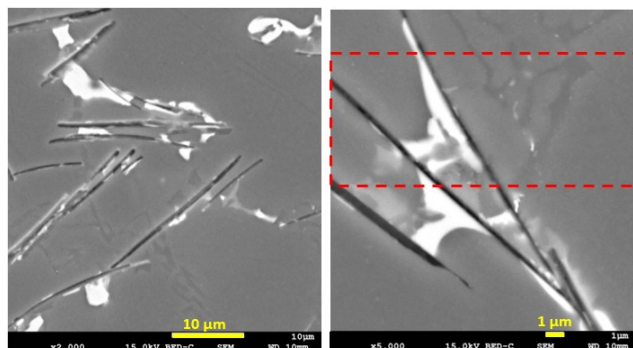


Fig. 7. Copper and iron rich area of precipitation, alloy after 5<sup>th</sup> remelting D5; SEM a) distribution of copper phases near iron needles b) detail of place of crystallization copper-rich phases

The red rectangle in the image shows the location of the line EDX analysis when magnified 5000 times (Fig. 7b). The analysis together with the mapping confirmed that the iron phase needles serve as nucleation areas in the monitored cases.

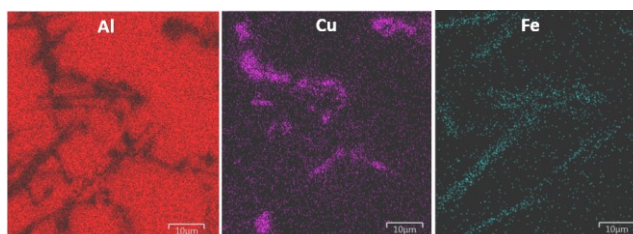


Fig. 8. Mapping of copper and iron rich area of precipitation; alloy after 5<sup>th</sup> remelting D5

In Al-Si-Cu-type alloys, copper-rich phases of Al<sub>2</sub>Cu type occur most frequently as well as in the presence of Fe type Al<sub>7</sub>FeCu. Samuel [11] states that the curable phases of Al<sub>2</sub>Cu can be eliminated in two forms, namely in the so-called "blocks" wherein the intermetallic compound contains about 40 wt. Cu %. The second form is a finely released eutectic containing about 24 wt. % copper released with aluminium. Based on the EDX analysis (Fig. 9), it can be concluded that the phase Al<sub>2</sub>Cu observed is released in the form of a fine eutectic.



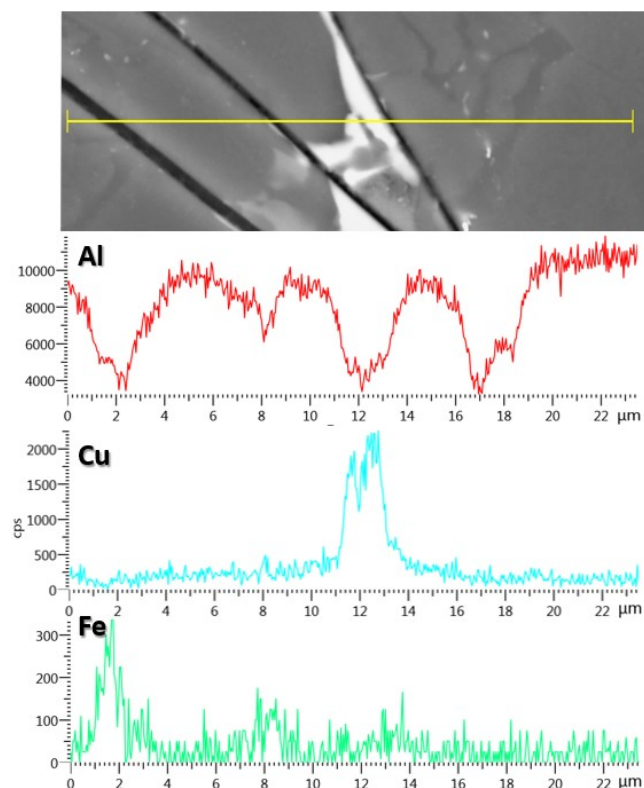


Fig. 9. Line EDX analysis of D5 alloy of copper and iron rich area of precipitation; alloy after 5<sup>th</sup> remelting D5

## 4. Conclusions

The theme of remelting is still very important today. The method and, in particular, the extent to which the use of the remelted material affects the resulting utility properties is a very important finding. Thanks to this finding, it is then possible to adjust the production so that the required quality of the casting is achieved at the highest possible consumption of the remelted or returnable material.

From the results obtained, it can be concluded that remelting and its effect were only partially reflected in the cooling curves and their first derivatives. The most significant change was noted in the crystallization of the iron-rich phases. An increase in nucleation temperature and an increase in the amount of latent heat can be attributed to the gradual increase in iron content in experimental alloys due to the application of multiple remelting. The remelting also caused slight changes in the copper content, which influenced the nucleation temperature of the copper phases.

Exceeding the critical iron content in each of the experimental alloys led to the formation of harmful iron phases prior to crystallization of the eutectic. The iron phases  $\beta$  -  $\text{Al}_5\text{FeSi}$  were observed exclusively in needle morphology. The length of the needles varied depending on the number of remelts. The shortest dimensions of the needles were measured for alloy D3 and the subsequent remelting increased the average lengths up to the

maximum values achieved by the alloy after the sixth remodeling of D7.

The copper-rich phases in all alloys were eliminated mainly around the needles of the iron phases. The most commonly observed phase was the curable phase  $\text{Al}_2\text{Cu}$ , released as a fine eutectic.

## Acknowledgement

This article was created as part of the VEGA grant agency: 1/0494/17. The authors hereby thank the Agency for their support.

## References

- [1] Matejka, M. & Bolibruchová, D. (2018). Effect of remelting on microstructure of the  $\text{AlSi9Cu3}$  alloy with higher iron content. *Archives of Foundry Engineering*. 18(4), 25-30.
- [2] Cao, X. & Campbell, J. (2006). Morphology of  $\text{Al}_5\text{FeSi}$  Phase in Al-Si Cast Alloys. *Materials Transactions*. 47(5), 1303-1312
- [3] Łągiewka, M., Konopka, Z., Zyska, A. & Nadolski, M. (2010). The influence of modification on the flow and the solidification of  $\text{AlSi10Mg}$  alloy. *Archives of Materials Science and Engineering*. 10(4), 119-122.
- [4] Grzincic, M., Dirnberger, F., Djurdjevic, M.B. (2012). *Application of the cooling curve analysis in aluminum casting plants*. Productive Operation of a Foundry. ISBN 978-80-02-024033.
- [5] Djurdjevic, M.B., Odanovic, Z. & Talijan, N. (2011). Characterization of the Solidification Path of  $\text{AlSi5Cu}(1-4 \text{ wt.}\%)$  Alloys Using Cooling Curve Analysis. *The Journal of The Minerals, Metals & Materials Society*. 63-11, 51-57
- [6] Taylor, J.A. (2012). Iron-containing intermetallic phases in Al-Si based casting alloys. *Procedia Materials Science*. 1, 19-33.
- [7] Tillová, E. & Panušková, M. (2008). Effect of solution treatment on intermetallic phases morphology in  $\text{AlSi9Cu3}$  cast alloy. *Metabk*. 47 (3), 207-210.
- [8] Matejka, M. & Bolibruchová, D. (2019). Application of Natural and Artificial Ageing on Multiply Remelted  $\text{AlSi9Cu3}$  Alloy. *Archives of Foundry Engineering*. 19(2), 60-66.
- [9] Marchwica, P. (2012). *Microstructural and Thermal Analysis of Aluminum-Silicon and Magnesium-Aluminum Alloys Subjected to High Cooling Rates*. Electronic Theses and Dissertations. 5572.
- [10] Emadi, L., Whiting, R., Schmid-Fetzer, (2008). Influence of Sn on Solidification Characteristics and Properties of  $\text{AlSiCuMg}$  Cast Alloys. Experimental and Thermodynamic Approaches, ICCA 11, Aachen, Germany. 328-335
- [11] Samuel, A.M., Doty, H.W., Samuel, F.H. (1996). Factors Controlling the Type and Morphology of Copper-Containing Phases in the 319 Aluminum Alloy. 100th AFS Casting Congress, Philadelphia, Pennsylvania, USA, April 20-23